Analytica Chimica Acta 909 (2016) 51–59

Contents lists available at ScienceDirect

Analytica Chimica Acta

journal homepage: www.elsevier.com/locate/aca

Covalent functionalization of single-walled carbon nanotubes with polytyrosine: Characterization and analytical applications for the sensitive quantification of polyphenols

Marcos Eguílaz [a], Alejandro Gutiérrez [a], Fabiana Gutierrez [a], Jose Miguel González-Domínguez [b, 1], Alejandro Ansón-Casaos [b], Javier Hernández-Ferrer [b], Nancy F. Ferreyra [a], María T. Martínez [b, **], Gustavo Rivas [a, *]

[a] INFIQC, Departamento de Fisicoquímica, Facultad de Ciencias Químicas, Ciudad Universitaria, 5000 Córdoba, Argentina
[b] Grupo de nanoestructuras de carbono y Nanotecnología, Departamento de Nanotecnología, Instituto de Carboquímica (CSIC), 50018 Zaragoza, Spain

HIGHLIGHTS

- Covalent modification of SWCNT with polytyrosine facilitates their dispersion.
- SWCNT-Polytyr is successfully deposited at GCE, at variance with GCE/SWCNT-ox.
- Oxidation of tyrosine residues offers an intrinsic signal to follow the presence of SWCNT at GCE.
- GCE/SWCNT-Polytyr allows the nanomolar detection of gallic acid.
- GCE/SWCNT-Polytyr is successfully used to quantify polyphenols in tea samples.

GRAPHICAL ABSTRACT

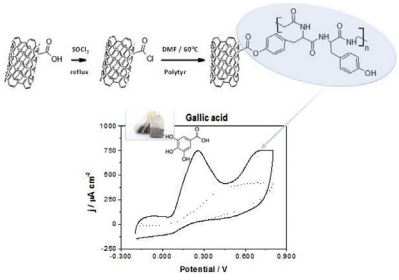

ARTICLE INFO

Article history:
Received 28 July 2015
Received in revised form
27 December 2015
Accepted 28 December 2015
Available online 5 January 2016

Keywords:
Single-walled carbon nanotubes
Covalent functionalization
Polytyrosine
Gallic acid

ABSTRACT

This work reports the synthesis and characterization of single-walled carbon nanotubes (SWCNT) covalently functionalized with polytyrosine (Polytyr); the critical analysis of the experimental conditions to obtain the efficient dispersion of the modified carbon nanotubes; and the analytical performance of glassy carbon electrodes (GCE) modified with the dispersion (GCE/SWCNT-Polytyr) for the highly sensitive quantification of polyphenols. Under the optimal conditions, the calibration plot for the amperometric response of gallic acid (GA) shows a linear range between 5.0×10^{-7} and 1.7×10^{-4} M, with a sensitivity of (518 ± 5) m AM^{-1} cm^{-2}, and a detection limit of 8.8 nM. The proposed sensor was successfully used for the determination of total polyphenolic content in tea extracts.

1. Introduction

The development of sensing methodologies for the detection/quantification of different analytes in a fast, sensitive, selective, and friendly way is one of the major challenges in Clinical Chemistry,

* Corresponding author.
** Corresponding author.
E-mail addresses: mtmartinez@icb.csic.es (M.T. Martínez), grivas@fcq.unc.edu.ar (G. Rivas).
[1] Current address: MSOC-Nanochemistry Group, Faculty of Chemistry, Universidad de Castilla-La Mancha, Avda. Camilo José Cela S/N, 13071 Ciudad Real, Spain.

http://dx.doi.org/10.1016/j.aca.2015.12.031
0003-2670/

food industry, environmental monitoring, and homeland security, among others [1–3]. Electrochemical (bio)sensors have demonstrated to be an interesting alternative, especially in the last years after the incorporation of new nanomaterials either to support the (bio)recognition layer, to improve the selectivity of the sensor assay, or to facilitate the signal transduction [4,5]. Among nanomaterials, carbon nanotubes (CNTs) have demonstrated to be an excellent component for the development of electrochemical (bio) sensors [6–8]. Their unique properties have made possible to obtain (bio)sensors with higher sensitivities, faster response times, lower working potentials, less surface fouling effects, and higher stability and robustness [9,10].

CNTs have a strong tendency to agglomerate via van der Waals forces or π–π stacking, making difficult their use in bio-related devices fields [11]. Therefore, new strategies that minimize these interactions are highly required for the development of CNTs-based electrochemical (bio)sensors [12–15]. In this sense, the covalent functionalization of CNTs represents an interesting alternative [16,17].

Here, we report the synthesis and characterization of single-walled carbon nanotubes (SWCNT) covalently functionalized with polytyrosine (Polytyr), and the analytical applications of glassy carbon electrodes (GCE) modified with the dispersion of SWCNT-Polytyr for the highly sensitive quantification of gallic acid (3,4,5-trihydroxy benzoic acid (GA)).

Due to their amphiphilic character, polypeptides have been successfully used as CNTs dispersing agents [18]. Higashi et al. [19] have reported the effect of the decoration of SWCNTs with Polytyr comparatively with dsDNA-decorated SWCNTs. Tsoufis et al. [20] have described the interaction of tyrosinate radical formed by Fenton's reagent with SWCNTs and have demonstrated that an unpaired electron can be localized and stabilized at the surface of CNTs. Kojima et al. [21] have reported the formation of SWCNT-Polytyr complexes by adsorption of Polytyr onto SWCNT walls. Recently [22], we have reported the immobilization of tyrosine and Polytyr at graphene nanoribbons obtained by oxidative unzipping of CNTs.

GA is one of the main natural phenolic compounds widely distributed in plants, humic substances, teas and wines [23–25] and possesses excellent medicinal properties as antimutagenic, anticarcinogenic, antioxidant, antiinflamatory, and heart disease protector [26,27]. Therefore, efficient sensing methodologies to quantify GA are highly required. In this sense, several electrochemical methods have been proposed for the quantification of GA, either based on the direct [28–35] or enzymatic [36–38] quantification using different (bio)sensors.

In the following sections we discuss the more relevant aspects of SWCNT-Polytyr synthesis; the characterization of the resulting functionalized nanostructures by FT-IR, TGA and cyclic voltammetry; the optimization of SWCNT-Polytyr dispersion; the comparison of the behavior of GCE/oxidized SWCNTs and GCE/SWCNT-Polytyr; and the analytical performance of GCE/SWCNT-Polytyr for the quantification of GA.

2. Experimental

2.1. Chemicals and solutions

Single walled carbon nanotubes (SWCNTs, AP-SWNT grade), were supplied from Carbon Solutions Inc. (Riverside, California). Hydrogen peroxide (30% v/v aqueous solution), ascorbic acid (AA), ethanol, NaH_2PO_4 and Na_2HPO_4 were purchased from Baker. Poly-L-Tyrosine (Polytyr), N,N-diisopropylethylamine (EDIPA), thionyl chloride, catechin (CA), gallic acid (GA), and tannic acid (TA) were purchased from Sigma. All chemicals were of analytical grade and used without further purification. The tea samples were obtained in a local store.

A 0.050 M phosphate buffer solution pH 7.40 was employed as supporting electrolyte. Ultrapure water (ρ = 18.2 MΩ cm) from a Millipore-MilliQ system was used for preparing all aqueous solutions. All the experiments were conducted at room temperature.

2.2. Apparatus

Fourier transform infrared spectroscopy (FTIR) measurements were performed with a Bruker Vertex 70 spectrometer. The samples were prepared with spectroscopic-grade KBr.

Thermogravimetric analysis (TGA) was carried out with a Setaram balance, model Setsys Evolution 16/18. The experiments were performed between room temperature and 800 °C using a heating ramp of 10 °C min^{-1} and 50 mL min^{-1} constant nitrogen flow.

Sonication treatments were carried out either with an ultrasonic processor VCX 130 W (Sonics and Materials, Inc.) of 20 kHz frequency containing a titanium alloy microtip (3 mm diameter) or an ultrasonic bath (TESTLAB, model TB04) of 40 kHz frequency and 160 W of nominal power. An Allegra™ 21 ultracentrifuge (Beckman Coulter) with a F2402H rotor was used to centrifuge the samples after sonication.

UV–vis absorption spectra were obtained with a Shimadzu UV-1700 Pharma spectrophotometer using a quartz cuvette of 1 mm path length. The samples were diluted 5 times before obtaining the corresponding spectra.

Scanning Electron Microscopy (SEM) images were obtained with a Field Emission Gun Scanning Electron Microscope (FE-SEM, Zeiss, ΣIGMA model) equipped with secondary and back-scattered electron detectors. The samples were prepared by depositing an aliquot of the dispersion onto GCE disks and drying by exposure to air.

Electrochemical experiments were carried out with a TEQ_04 potentiostat. Unmodified glassy carbon electrodes (GCE, CH Instruments, 3 mm diameter) and glassy carbon electrodes modified with a dispersion of SWCNT covalently functionalized with Polytyr (SWCNT-Polytyr) were used as working electrodes. A platinum wire and Ag/AgCl, 3 M NaCl (BAS, Model RE-5B) were used as auxiliary and reference electrodes, respectively. All potentials are referred to this reference electrode. A magnetic stirrer under controlled speed provided the convective transport during the amperometric measurements.

2.3. Synthesis of functionalized SWCNT

SWCNT were purified by air oxidation at 350 °C for 2 h and further reflux in 3 M HCl for 2 h. The resulting nanostructures were oxidized by a reflux for 3 h in a 3 M H_2SO_4/HNO_3 mixture 50:50 v/v (SWCNT-ox). Once filtered, rinsed with deionized water and over-dried, the solid was functionalized with Polytyr (SWCNT-Polytyr). In a typical experiment, 120 mg of SWCNTs-ox were placed in a round-bottom flask and dispersed in 10 mL of anhydrous *N*,*N*′-dimethylformamide (DMF), using an ultrasound bath for 30 min. Then, 24 mL of thionyl chloride were carefully added, and the resulting mixture was refluxed at 120 °C for 24 h with constant magnetic stirring. The product was them vacumm-filtrated through a 0.1 μm pore size Teflon membrane, thoroughly washed with anhydrous tetrahydrofuran and dried in vacumm at room temperature to obtain acyl chloride-SWCNTs. A portion of 100 mg of the freshly acylated SWCNTs was dispersed in 25 mL of anhydrous DMF with ultrasound bath while the flask was purged with a continuous Ar flow. The reaction continued with the addition of 2 mL EDIPA and 8 mg Polytyr. The mixture was allowed to react at

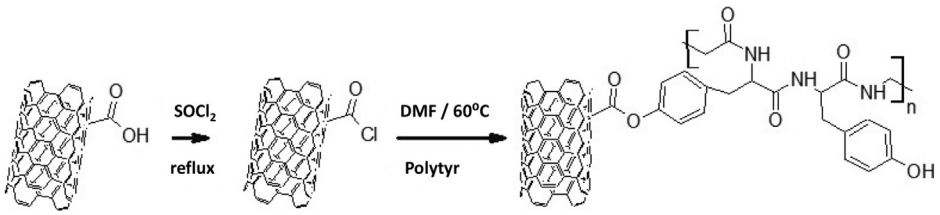

Scheme 1. Scheme of the covalent functionalization of SWCNT with Polytyr.

60 °C for four days under Ar atmosphere (Scheme 1).

2.4. Preparation of GCE modified with SWCNT-Polytyr

2.4.1. Preparation of the SWCNT-Polytyr dispersion

SWCNTs-Polytyr dispersions were prepared by mixing 1.0 mg of SWCNT-Polytyr with 1.0 mL of 50:50% v/v ethanol/water solution followed by sonication with a sonicator probe for 10.0 min using 50% amplitude and keeping the sample in an ice-bath during the procedure. After this treatment, the samples were centrifuged at 9000 rpm for 15 min and the supernatant was collected for further work. For comparison, SWCNT-ox were dispersed in a similar way.

2.4.2. Preparation of GCE modified with SWCNTs-Polytyr dispersion (GCE/SWCNT-Polytyr)

GCE surfaces were polished with alumina slurries of 1.0, 0.3 and 0.05 μm for 1 min each, rinsed thoroughly with deionized water, sonicated for 30 s in water, and finally dried under a nitrogen stream. GCE/SWCNT-Polytyr was prepared by casting 10 μL of the supernatant obtained after centrifuging the SWCNT-Polytyr dispersion onto the GCE surface. The solvent was allowed to evaporate at room temperature for 30 min. GCE/SWCNT-ox was prepared following a similar scheme using SWCNT-ox instead of SWCNT-Polytyr.

2.5. Procedure

Cyclic voltammetry (CV) was carried out between −0.200 V and 0.800 V at a scan rate of 0.100 Vs^{-1}. Amperometric experiments were performed in stirred solutions by applying the desired working potential and allowing the transient current to reach a steady-state value prior to the addition of the analyte and the subsequent current monitoring. All the experiments were conducted at room temperature. With exception of the calibration plot, all the results presented here were obtained using three different electrodes. In the case of the calibration plot each point represents the average of the results obtained with five dispersions and three different electrodes per dispersion.

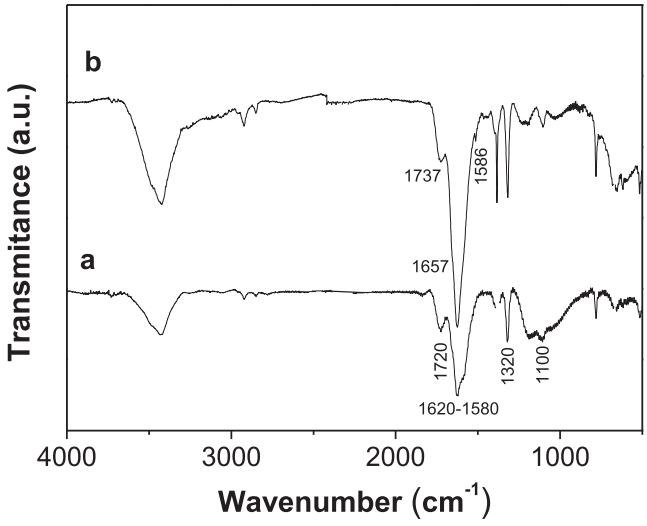

Fig. 1. FT-IR spectra for: (a) SWCNT-ox, (b) SWCNT-Polytyr.

2.6. Determination of total polyphenolic content in tea extracts

2.6.1. Preparation of tea extracts

Green (*Patagonia*), red (*Patagonia*), classic (*Green Hill*) and herbal

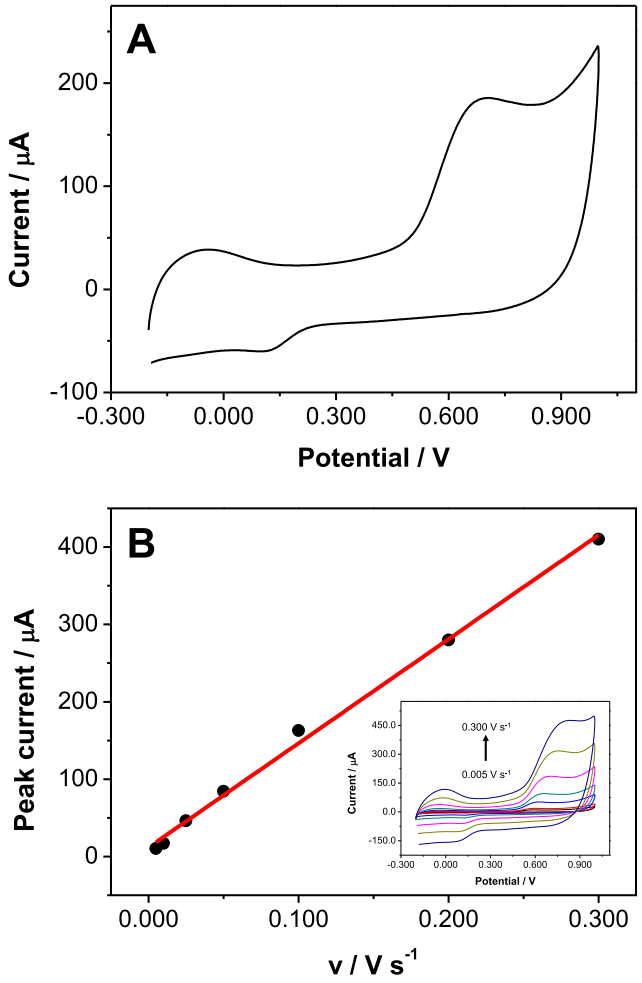

Fig. 2. (A) Cyclic voltammogram obtained at GCE/SWCNT-Polytyr in a solution of 0.050 M phosphate buffer solution pH 7.40. v = 0.100 Vs^{-1}. Dispersion conditions: 1.0 mg mL^{-1} SWCNT-Polytyr in 50/50% v/v ethanol/water using an ultrasonic tip. Sonication time: 10.0 min, acoustic amplitude 50%. Centrifugation at 9000 rpm for 15.0 min. (B) Dependence of oxidation peak currents on the scan rates. Inset: Cyclic voltammograms of the GCE/SWCNTs-Polytyr at different scan rates.

(*Taragüí*) teas were used for testing the analytical performance of the proposed sensor in real samples. Briefly, tea infusions were prepared by adding 70 mL of boiling MilliQ water to the full content of the tea-bag (2.000 g with exception of the herbal tea where the content was 1.500 g), and stirred for 30 min. The collected extracts were centrifuged at 2000 rpm for 5.0 min and cooled down at room temperature. The obtained supernatants were protected with aluminum foil and kept in refrigerator until use.

2.6.2. Determination of total polyphenolic content (TPC) using the SWCNT-Polytyr

The TPC of tea samples was determined with the GCE/SWCNT-Polytyr sensor by amperometry at 0.200 V. The experiments were performed by addition of the tea aliquot to 5.00 mL of a 0.050 phosphate buffer solution pH 7.40. The determination was performed using the standard additions method and GA as standard. TPC was expressed as g of GA equivalent per 100 g of dried tea sample (%GAE) and the values were taken as the average of three determinations.

3. Results and discussion

3.1. Characterization of SWCNT-Polytyr

Fig. 1 displays FTIR spectra for SWCNT-ox (a) and SWCNT-Polytyr (b). The spectrum for SWCNT-ox shows bands characteristics of the oxygenated groups generated during the oxidation process, typically at 1100 cm^{-1} (C–O stretching), 1320 cm^{-1} (O–H stretching), and 1580–1620 cm^{-1} and 1720 cm^{-1} (carboxylate) [39]. After functionalization of SWCNT-ox the number of bands greatly enhances in the region between 1550 and 1750 cm^{-1}. The covalent attachment of Polytyr was evidenced from the appearance of new bands between 1500 and 1600 cm^{-1} due to the formation of amide bonds: at 1586 cm^{-1} (bending vibration N–H, Amide II) and at 1657 cm^{-1} (C=O stretching vibration, Amide

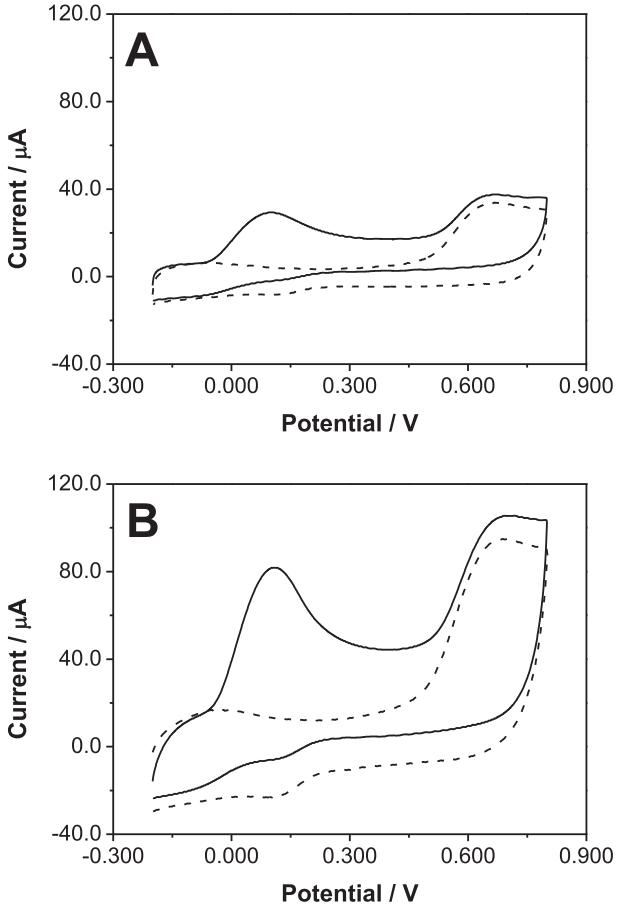

Fig. 3. Cyclic voltammograms obtained in the presence (solid line) and absence (dashed line) of 1.0×10^{-3} M AA at GCE modified with dispersions of 1.0 mg mL^{-1} SWCNT-Polytyr in (A) water and (B) 50/50% v/v ethanol/water using an ultrasonic tip. Supporting electrolyte: 0.050 M phosphate buffer solution pH 7.40. Sonication time: 5.0 min, acoustic amplitude 50% and centrifugation at 9000 rpm for 15.0 min. v = 0.100 Vs^{-1}.

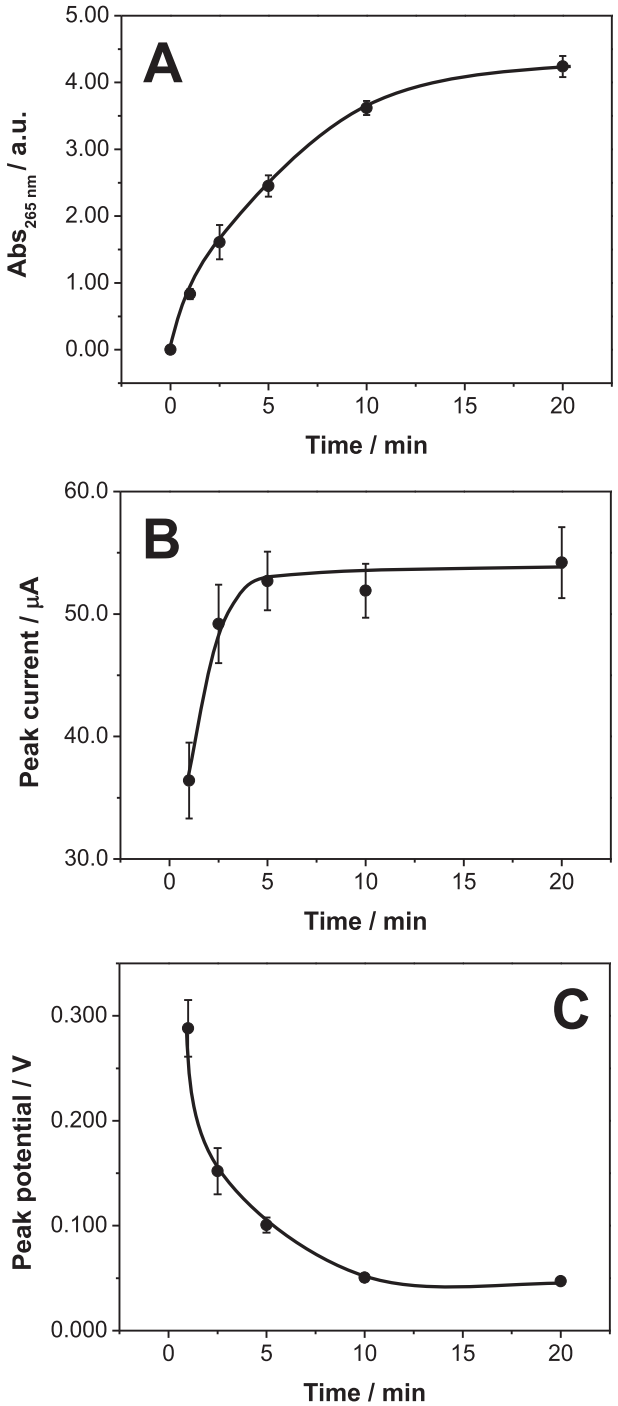

Fig. 4. Effect of the sonication time of SWCNT-Polytyr dispersion on the absorbances at 265 nm (A); and the peak current (B) and peak potential (C) for the oxidation of 1.0×10^{-3} M AA obtained at GCE modified with SWCNT-Polytyr dispersions prepared in 50/50% v/v ethanol/water with different sonication time. v = 0.100 Vs^{-1}. Other conditions as in Fig. 3.

I) [40]. One additional band appears at 1737 cm^{-1} (C═O stretching ester), consistent with the ester functional groups present in the Polytyr.

The attachment of Polytyr at SWCNT surface was also evaluated by TGA. Figure 1-SI (Supplementary Information) depicts the TGA plots for SWCNT treated in air-HCl (a), SWCNT-ox (b) and SWCNT-Polytyr (c). There is a slight weight loss up to 100 °C, which corresponds to the residual moisture present in the SWCNT samples. This moisture content is especially evident in the case of SWCNT-ox and SWCNT-Polytyr samples, consistent with their higher hydrophilicity. The thermal stability of SWCNT-Polytyr is visibly higher than that of SWCNT-ox, since the functionalization process involves an important loss of oxygenated functional groups as it was reported for the functionalization of graphene nanoribbons with Polytyr [22].

Fig. 2A shows a potentiodynamic profile obtained at GCE/SWCNT-Polytyr in a 0.050 M phosphate buffer solution pH 7.40 at 0.100 Vs^{-1}. There is a current peak at 0.70 V due to the irreversible oxidation of tyrosine residues [22,41]. The peak currents depend linearly on the scan rate between 0.005 and 0.300 Vs^{-1}, demonstrating that the oxidation of tyrosine residues is a surface-controlled process (Fig. 2B). These results represent another evidence of the presence of tyrosine residues at the electrode surface.

3.2. Optimization of SWCNT-Polytyr dispersion

The optimization of the conditions for dispersing SWCNT-Polytyr was performed through the evaluation of the voltammetric parameters for the oxidation of the redox marker AA and the absorbance at 265 nm (Abs_{265}), taking into account that individual

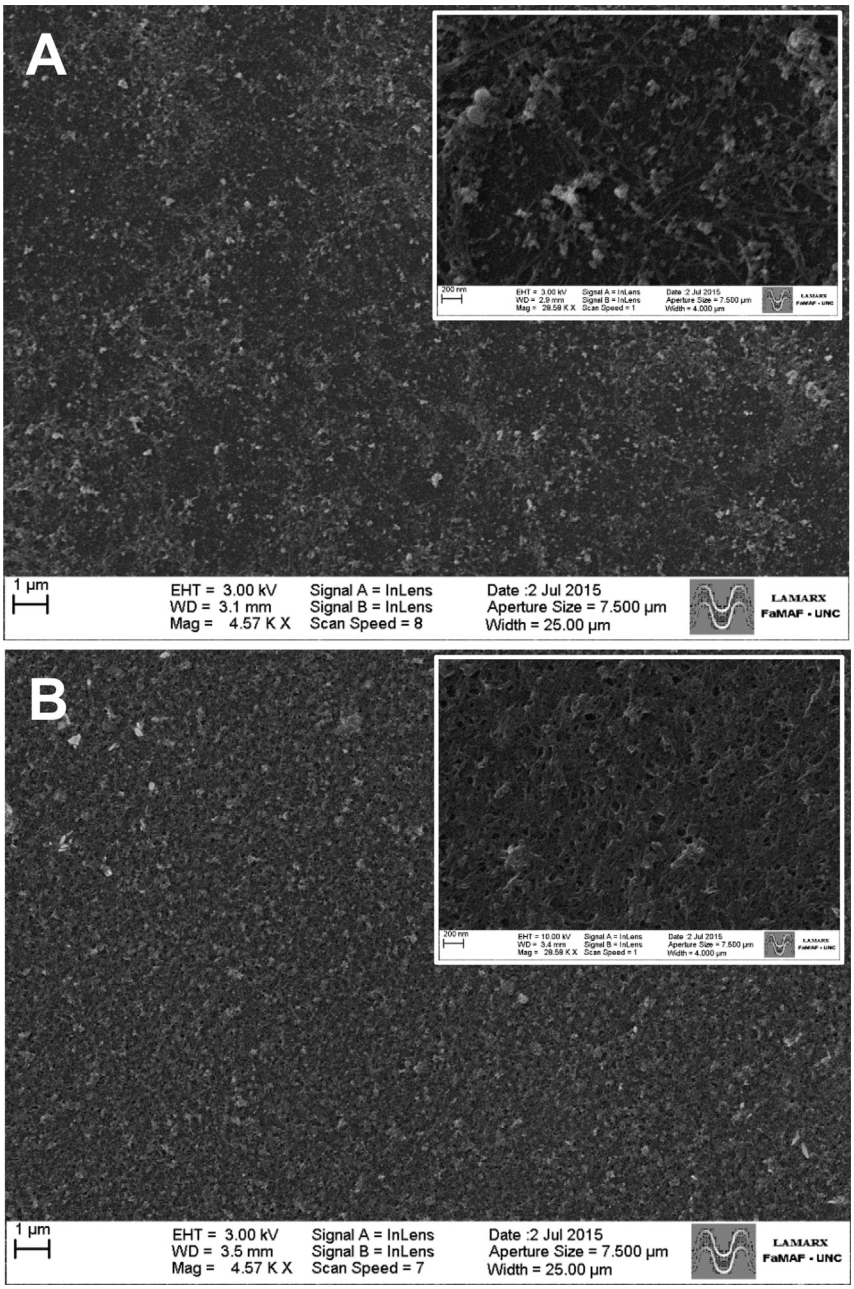

Fig. 5. SEM micrographs of glassy carbon disks modified with dispersions of SWCNT-ox (A) and SWCNT-Polytyr (B) prepared in 50/50% v/v ethanol/water. Magnification: 5470×. The insets correspond to pictures of the same disks obtained with higher magnification (28590×). Other conditions as in Fig. 3.

nanotubes strongly absorb at 265 nm due to the $\pi-\pi^*$ transition of aromatic sp^2 and to the increase of the absorbance by dispersing the SWCNT aggregates [42–45].

Fig. 3 displays cyclic voltammograms for 1.0×10^{-3} M AA at GCE modified with SWCNT-Polytyr dispersions prepared in water (A) and 50/50% v/v ethanol/water (B). The comparison of both profiles indicate that the oxidation peak potentials (E_p) at both glassy carbon modified electrodes are very close (0.100 V (A) vs 0.103 V (B)) and that the oxidation peak currents (i_p) increase in a factor of 2.5 at glassy carbon modified with SWCNT-Polytyr prepared in ethanol/water. The analysis of the i-E profiles obtained in phosphate buffer solution (shown in dotted line) indicates that at GCE modified with SWCNT-Polytyr dispersed in ethanol/water, the capacitive currents largely increase and the peak current for the oxidation of tyrosine residues increases almost in a factor of 3. The Abs_{265} largely increased when the solvent used to prepare the dispersion was ethanol/water (absorbances of 0.178 and 0.521 for the dispersions prepared in water and ethanol/water, respectively, using 5.0 min sonication).

In summary, the increase in the Abs_{265} observed when dispersing SWCNT-Polytyr in ethanol/water, and the increment in the capacitive currents and peak currents for tyrosine and AA oxidation obtained at GCE/SWCNT-Polytyr (in ethanol/water), indicate that the amount of disaggregated SWCNT-Polytyr increases when using ethanol/water instead of water. In addition, the stability of the dispersion was better when using the ethanol/water solution. Thus, the selected solvent for preparing the dispersion was 50/50% v/v ethanol/water.

The amount of SWCNT-Polytyr dispersed in 50/50%v/v ethanol/water was optimized using the Abs_{265} and the AA oxidation peak current as indicators (Fig. 2-SI). In all cases the sonication time was 5.0 min and the dispersion was centrifuged at 9000 rpm for 15.0 min. The Abs_{265} increased with the amount of SWCNT-Polytyr in the dispersion from 0.50 to 1.00 mg mL^{-1} to slightly decrease thereafter. In agreement with these results, cyclic voltammetry profiles for 1.0×10^{-3} M AA at GCE modified with SWCNT-Polytyr dispersions prepared with different amount of CNTs demonstrated

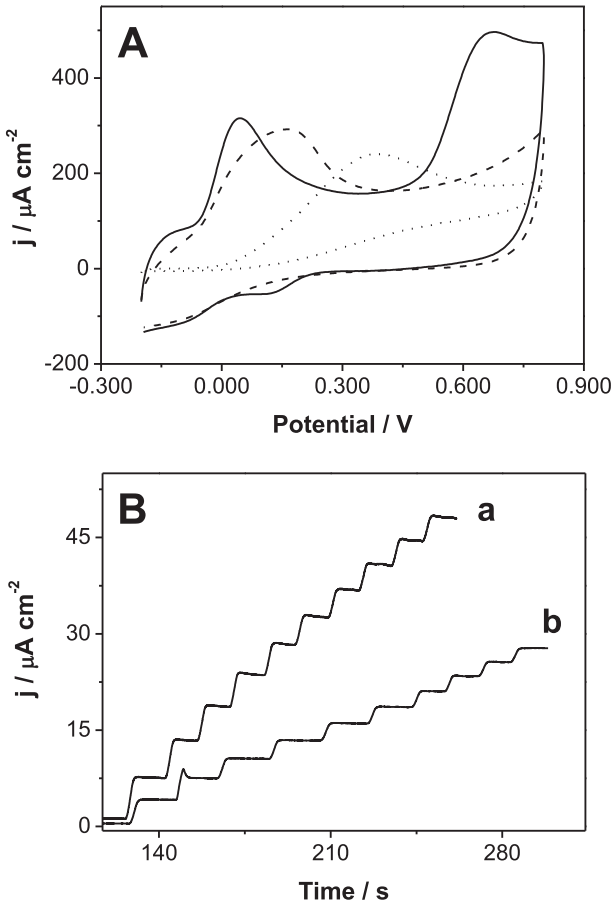

Fig. 6. (A) Cyclic voltammograms for 1.0×10^{-3} M AA at bare GCE (dotted line), GCE/SWCNT-ox (dashed line) and GCE/SWCNT-Polytyr (solid line). $v = 0.100$ Vs^{-1}. (B) Amperometric response at 0.500 V obtained for successive additions of 1.0×10^{-3} M H_2O_2 at GCE/SWCNT-Polytyr (a) and GCE/SWCNT-ox (b). Other conditions as in Fig. 3.

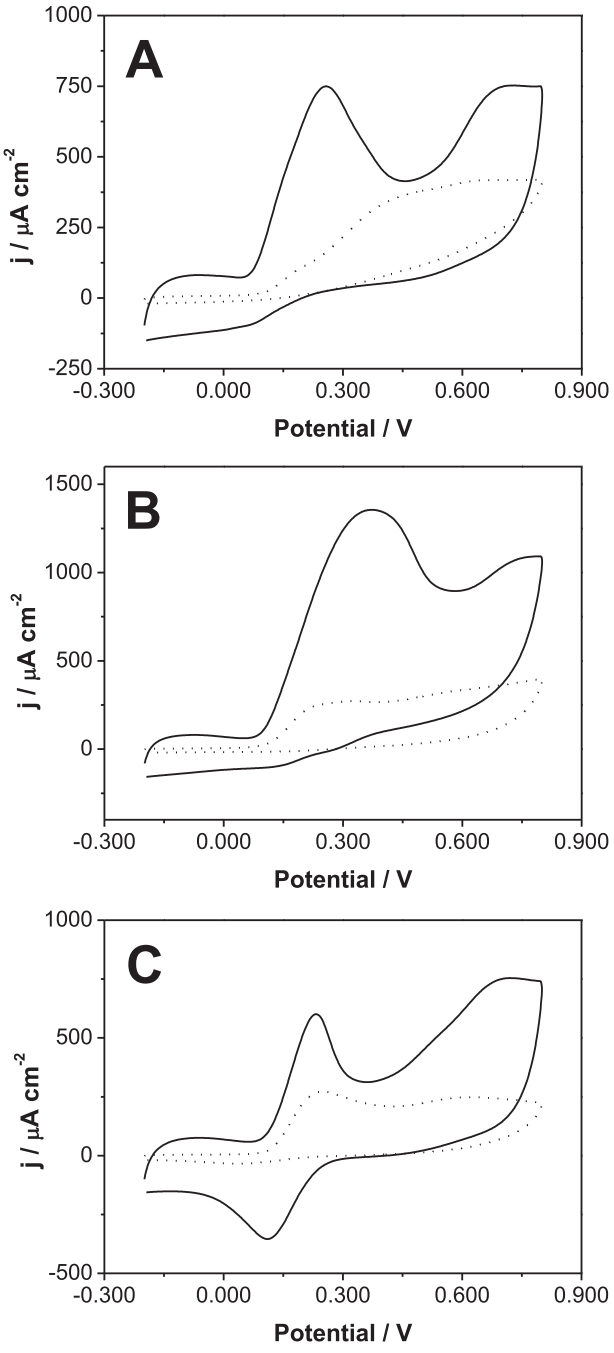

Fig. 7. Cyclic voltammograms for (A) 1.0×10^{-3} M gallic acid, (B) 1.0×10^{-3} M tannic acid and (C) 1.0×10^{-3} M catechin at bare GCE (dotted line) and GCE/SWCNTs-Polytyr (solid line). $v = 0.100$ Vs^{-1}. Other conditions as in Fig. 3.

that i_p for AA oxidation increases with the amount of SWCNT-Polytyr up to 1.00 mg mL^{-1}. Therefore, spectrophotometric and electrochemical results demonstrated that the maximum amount of SWCNT-Polytyr that can be efficiently disaggregated under these experimental conditions is 1.0 mg mL^{-1}.

As it is known [12], the sonication time is a critical parameter when dispersing carbon nanotubes since a chain of cavitation events have to be produced to ensure the separation of the nanotubes. We studied the effect of the sonication time on the dispersion of 1.0 mg mL^{-1} SWCNT-Polytyr (centrifuged at 9000 rpm for 15.0 min) from the changes in Abs_{265} and from E_p and i_p for 1.0×10^{-3} M AA electro-oxidation. Fig. 4A shows that Abs_{265} increases up to 10.0 min sonication, to remain almost constant thereafter. Fig. 4B and C displays the variation of the AA voltammetric parameters with the sonication time of the dispersion used to modify the GCE. The i_p for AA oxidation increases with the increment in the sonication time up to 5.0 min, to keep constant for longer times (Fig. 4B). An interesting profile is obtained for the variation of AA oxidation peak potential with the sonication time, since it largely decreases with the increase of the sonication time up to 10.0 min, to remain almost constant for longer times (Fig. 4C). These results indicate that the disaggregation of SWCNT-Polytyr improves with the increment of the sonication time and that after a critical time, 10.0 min in this case, the exfoliation of SWCNT-Polytyr reaches its maximum efficiency. Hence, the selected value was 10.0 min.

The advantages of the covalent attachment of Polytyr to SWCNT-ox for further development of electrochemical sensors was also studied. We evaluate these advantages by comparing: i) Abs_{265} of SWCNT-ox and SWCNT-Polytyr dispersions prepared in 50/50%v/v ethanol/water, ii) SEM images of glassy carbon disks covered with SWCNT-ox and SWCNT-Polytyr dispersions, iii) the voltammetric profiles for 1.0×10^{-3} M AA oxidation at GCE/SWCNT-ox and GCE/SWCNT-Polytyr, and iv) the amperometric response of hydrogen peroxide at GCE modified with both dispersions.

Abs_{265} for SWCNT-Polytyr was around 15% higher than the one obtained for analogous dispersions containing SWCNT-ox, suggesting that no significant changes were produced in the disaggregation of SWCNTs (not shown).

SEM images for GCE/SWCNT-ox (A) and GCE/SWCNT-Polytyr (B) are shown in Fig. 5. The insets display pictures of the same surfaces obtained with higher magnification. The analysis of the different images demonstrates that SWCNT-ox (A) does not cover the electrode surface in an homogeneous way, delimiting areas with poor coverage, at variance with SWCNT-Polytyr (B) where the coverage was excellent. These results strongly suggest that the presence of the polymer facilitates the deposition of the nanostructures at the glassy carbon surfaces.

Fig. 6A depicts the potentiodynamic profiles for 1.0×10^{-3} M AA at bare GCE (dotted line), GCE/SWCNT-ox (dashed line) and GCE/SWCNT-Polytyr (solid line). The presence of SWCNTox or SWCNT-Polytyr at the electrode surface, largely improves the electrooxidation of AA, although the most drastic change in the overvoltage for AA oxidation was attained at GCE/SWCNT-Polytyr (E_p = 0.385, 0.160 and 0.045 V at GCE, GCE/SWCNT-ox and GCE/SWCNT-Polytyr, respectively). In addition, while a well-defined current peak is observed at GCE/SWCNT-Polytyr, at GCE/SWCNT-ox the current peak for AA oxidation is very broad and shows more than one contribution. Similar behavior was observed for uric acid and dopamine (not shown).

Fig. 6B displays the amperometric response of hydrogen peroxide at 0.500 V for successive additions of 1.0×10^{-3} M hydrogen peroxide. The sensitivities obtained at GCE/SWCNT-ox and GCE/SWCNT-Polytyr were 3.5 and 6.0 mA M^{-1} cm^{-2}, respectively, demonstrating that, as in the case of AA, the covalent attachment of Polytyr to SWCNT-ox clearly improves the deposition of the nanostructures at GCE and further electroactivity of the resulting modified electrodes.

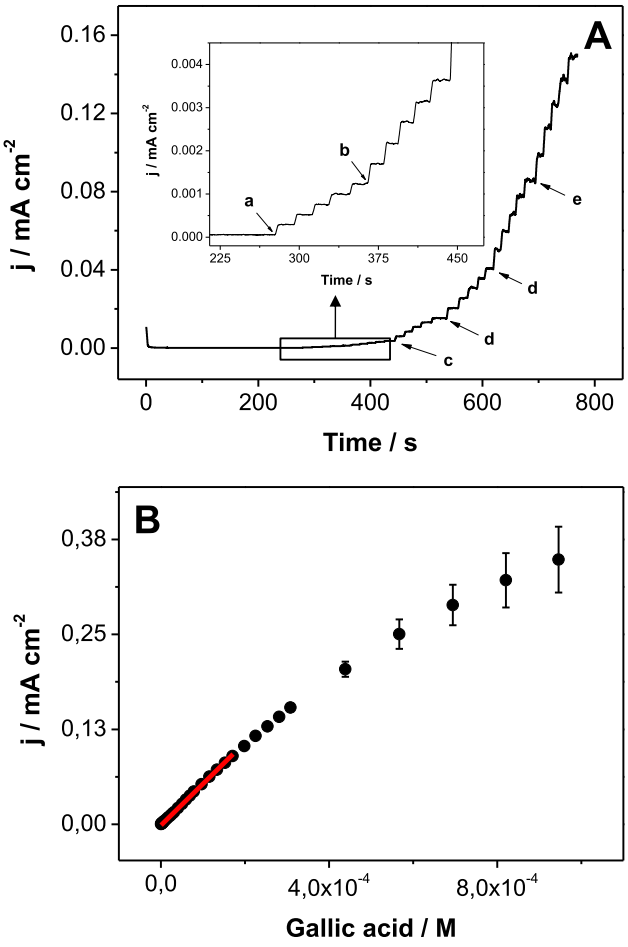

Fig. 8. (A) Amperometric recording obtained at GCE/SWCNT-Polytyr for successive additions of gallic acid: (a) 5.0×10^{-7} M, (b) 1.0×10^{-6} M, (c) 5.0×10^{-6} M, (d) 1.0×10^{-5} M, (e) 2.0×10^{-5} M, (f) 3.0×10^{-5} M. (B) Calibration plot obtained from the amperometric recording shown in Fig. 8A. Working potential: 0.200 V. Other conditions as in Fig. 3.

Therefore, the use of SWCNT-Polytyr instead of SWCNT-ox to modify GCE allowed a more efficient modification of the glassy carbon surfaces making possible a facilitated charge transfer for different redox markers and better definition of the associated voltammetric signals.

3.3. Analytical applications of GCE/SWCNT-Polytyr for GA quantification

Fig. 7 depicts cyclic voltammograms for 1.0×10^{-3} M GA (A), TA (B) and CA (C) at GCE (dotted line) and GCE/SWCNT-Polytyr (solid line) at 0.100 V s^{-1}. The comparison of the potentiodynamic profiles for GA at both electrodes demonstrated that at GCE/SWCNT-Polytyr

Table 1
Total polyphenolic content in tea samples.

Sample	TPC (% GAE)	RSD (%)
Green tea	12.3 ± 0.3	2.5
Red tea	4.4 ± 0.2	4.6
Classic tea	2.8 ± 0.1	5.0
Herbal tea	1.01 ± 0.05	5.2

Table 2
Analytical parameters for GA quantification obtained with different sensors or sensing methodologies.

Method	Linear range (M)	Limit of detection (M)	Sensitivity (mA M^{-1})	Reference
CPE/SiO_2NPs	8.00×10^{-7}–1.00×10^{-4}	2.50×10^{-7}	1.79	[48]
CPE/TiO_2NPs	5.00×10^{-6}–1.50×10^{-5}	9.40×10^{-7}	0.99	[49]
GCE/LDHf	4.00×10^{-6}–6.00×10^{-4}	1.60×10^{-6}	14.7	[50]
GCE/MIP/Ppy	1.00×10^{-4}–2.00×10^{-3}	–	0.041	[51]
GCE/PEP	1.00×10^{-6}–2.00×10^{-5}	6.63×10^{-7}	–	[52]
GrE/Th/NiHCF	4.99×10^{-6}–1.20×10^{-3}	1.66×10^{-6}	–	[53]
CPE/MWCNTs	5.00×10^{-7}–1.50×10^{-5}	3.00×10^{-7}	827.0	[54]
CPE/MWCNTs	6.25×10^{-6}–3.37×10^{-5}	2.00×10^{-7}	0.111	[55]
GCE/Gr-PEI	5.87×10^{-7}–5.87×10^{-5}	4.11×10^{-7}	2.16	[56]
SPE/MWCNTs/Lac	5.88×10^{-7}–1.06×10^{-4}	1.76×10^{-6}	1.19	[57]
GCE/CNT-NH_2/AuNPs/Lac-BSA	3.00×10^{-6}–6.00×10^{-5}	7.10×10^{-7}	169.0	[58]
ITO/PANI-rGO-TiO_2	4.17×10^{-6}–2.50×10^{-4}	1.72×10^{-6}	–	[59]
Flow-injection system and SPE	2.94×10^{-5}–1.47×10^{-4}	5.88×10^{-6}	–	[60]
Diffuse reflectance spectrometry	1.17×10^{-6}–3.50×10^{-5}	–	–	[61]
Capillary electrophoresis	1.39×10^{-5}–4.23×10^{-4}	1.17×10^{-5}	2.18	[62]
HPLC	1.54×10^{-5}–1.23×10^{-4}	2.18×10^{-6}	–	[63]
GCE/SWCNTs-Polytyr	5.00×10^{-7}–1.70×10^{-4}	8.8×10^{-9}	163.2	This work

AuNPs, gold nanoparticles; BSA, bovine serum albumine; CPE, carbon paste electrode; GCE, glassy carbon electrode; Gr, graphene; GrE, graphite electrode; ITO, indium tin oxide; Lac, laccase; LDHf, Zn–Al–NO_3 layered double hydroxide film; MIP, molecularly imprinted polymers; MWCNTs, multiwalled carbon nanotubes; NiHCF, Nickel hexacyanoferrate; PANI, polyaniline; PEI, polyethyleneimine; PEP, polyepinephrine; Polytyr, polytyrosine; Ppy, polypyrrole; rGO, reduced graphene oxide; SiO_2NPs, silica nanoparticles; SPE, screen printed electrode; SWCNTs, single walled carbon nanotubes; Th, thionine; TiO_2NPs, titanium dioxide nanoparticles.

there is a decrease of 200 mV in the oxidation overvoltage and an enhancement of two-fold in the oxidation peak current, clearly demonstrating the effect of the catalytic activity of SWCNT-Polytyr on the oxidation of GA. Cyclic voltammograms for TA (Fig. 7B) show a significant increase in the oxidation peak current, from 265 μA cm^{-2} at bare GCE to 1294 μA cm^{-2} at GCE/SWCNT-Polytyr. Finally, in the case of CA (Fig. 7C) the voltammetric profiles show a drastic change, from an irreversible behavior at bare GCE to a quasi-reversible behavior at GCE/SWCNT-Polytyr. In fact, the peak potential separation (ΔE_p) is 0.115 V, the oxidation peak current increases from 267 to 543 μA cm^{-2} and the reduction peak current, almost zero at bare GCE, is 325 μA cm^{-2} at GCE/SWCNT-Polytyr, defining a peak currents ratio (i_{pc}/i_{pa}) of 0.60. It is important to mention that no changes in the cyclic voltammetry profiles of CA were observed when the cyclic voltammogram was performed up to 0.400 V instead of 0.900 V, demonstrating that the changes observed in the reduction of CA oxidation product is not due to the Polytyr oxidation product.

Fig. 8A displays the amperometric response of GA at GCE/SWCNT-Polytyr. A clearly defined and fast response is observed after each addition of GA, even for concentrations as low as 5.0×10^{-7} M, with steady-state currents reached in 3 s. The calibration plot presented in Fig. 8B shows a wide linear range, from 5.0×10^{-7} M to 1.7×10^{-4} M, with a sensitivity of (518 ± 5) m $AM^{-1}cm^{-2}$ (or 163 ± 2 mAM^{-1}), $r^2 = 0.9992$, and a detection limit of 8.8 nM or 1.5 μgL^{-1} (taken as 3.3 σ/S, where σ is the standard deviation of the blank signal and S, the sensitivity).

The repeatability of the sensor was 6.5% (n = 5). The reproducibility was 1.9% using the same SWCNT-Polytyr dispersion and 5 different electrodes, and 3.1% using 5 different dispersions and three electrodes per dispersion.

The GCE/SWCNTs-Polytyr was used to quantify the TPC in different tea samples. Table 1 displays the TPC informed as %GAE for a green tea, red tea, classic tea and herbal infusion. Very good precision was obtained in all cases, demonstrating that the proposed sensing methodology represents a new alternative for the simple and fast electrochemical determination of total polyphenols, without needing of enzymes or additional markers.

The content of polyphenols in the tea samples was also determined by Folin-Ciocalteau method, although the results were not comparable to those obtained using the proposed electrochemical sensor, in agreement with other authors [46,47]. The explanation for this discrepancy is that the Folin-Ciocalteau reagent can react not only with di- or poly-phenols, but also with all the phenols and other non-phenolic organic compounds like sugars and proteins.

Table 2 summarizes the analytical parameters of different sensors or sensing methodologies to quantify GA reported in the last years. It is evident that the analytical performance of our sensor is highly competitive since it presents one of the lowest detection limits and the widest linear range. Regarding sensitivity, even when an strict comparison is not possible to do due to the lack of information about the areas of the other electrodes, the sensitivity obtained here is only smaller than the one obtained at CPE/MWCNTs [54], comparable to the one reported for GCE modified with amino-CNTs, Au NPs and laccase [58] and higher than those obtained with the other sensing methodologies.

4. Conclusions

The work reported here demonstrated the advantages of the covalent functionalization of SWCNT with a polymer rich in electroactive groups, like Polytyr. The polymer facilitates the dispersion of the CNTs and further deposition of the resulting dispersions at the glassy carbon surface, while the tyrosine residues allow to follow the presence of the CNTs at the electrode surface. The GCE/SWCNT-Polytyr demonstrated to be a highly sensitive sensor for GA useful for the successful quantification of polyphenols in tea samples.

The new functionalization scheme represents an alternative with an enormous potential for the development of different biosensors, not only based on the activity of SWCNT but also on the catalytic properties of the oxidation products of tyrosine without needing to incorporate additional mediators. We are currently working on this direction.

Acknowledgements

The authors thank Spanish MINECO (PRI-PIBAR-2011-1), the Government of Aragon (Project DGA-ESF-T66 CNN), the European Social Fund (ESF), CONICET, SECyT-UNC, MINCyT-Córdoba, ANPCyT (PICT 2010-1549 and PICT MICINN 2011-2748) for the financial support. M.E. and A. G. acknowledge CONICET for the fellowships.

Appendix A. Supplementary data

Supplementary data related to this article can be found at http://dx.doi.org/10.1016/j.aca.2015.12.031.

References

[1] C.I.L. Justiono, T.A. Rocha-Santos, A.C. Duarte, T.A. Rocha-Santos, Trends Anal. Chem. 87 (2015) 230–249.
[2] D.W. Kimmel, G. Le Blanc, M.E. Meschievitz, D.E. Cliffel, Anal. Chem. 84 (2012) 685–707.
[3] M. Labib, M.V. Berezovski, Biosens. Bioelectron. 68 (2015) 83–94.
[4] S. Kumar, W. Ahlawat, R. Kumar, N. Dilbaghi, Biosens. Bioelectron. 70 (2015) 498–503.
[5] C. Zhu, G. Yang, H. Li, D. Du, Y. Lin, Anal. Chem. 87 (2015) 230–249.
[6] N. Yang, X. Chen, T. Ren, P. Zhang, D. Yang, Sensors Actuat. B. Chem. 207 (2015) 690–715.
[7] A.M. Münzer, Z.R. Michael, A. Star, ACS Nano 7 (2013) 7448–7453.
[8] I. Willner, B. Willner, Nano Lett. 10 (2010) 3805–3815.
[9] N. Yang, X. Chen, T. Ren, P. Zhang, D. Yang, Sensors Actuat. B Chem. 207 (2015) 690.
[10] Z. Wang, Z. Dai, Nanoscale (**7**, 2015), 6420-6431.
[11] G.A. Rivas, M.D. Rubianes, M.C. Rodríguez, N.F. Ferreyra, G.L. Luque, M.L. Pedano, S.A. Miscoria, C. Parrado, Talanta 74 (2007) 291–307.
[12] E.N. Primo, F.A. Gutierrez, G.L. Luque, P.R. Dalmasso, A. Gasnier, Y. Jalit, M. Moreno, M.V. Bracamonte, M. Eguílaz, M.L. Pedano, M.C. Rodríguez, N.F. Ferreyra, M.D. Rubianes, S. Bollo, G.A. Rivas, Anal. Chim. Acta 805 (2013) 19–35.
[13] E.N. Primo, P. Cañete-Rosales, S. Bollo, M.D. Rubianes, G.A. Rivas, Colloid. Surf. B. Biointerfaces 108 (2013) 329–336.
[14] C. Garc, Z. Guo, J.-H. Liu, X.-J. Huang, Nanoscale 4 (2012) 1948–1963.
[15] P.-C. Ma, N.A. Siddiqui, G. Marom, J.-K. Kim, Compos. Part A Appl. Sci. Manuf. 41 (2010) 1345–1367.
[16] A. Hirsch, O. Vostrowsky, Top. Curr. Chem. 245 (2005) 193–237.
[17] A. Gasnier, J.M. González-Domínguez, A. Ansón-Casaos, J. Hernández-Ferrer, M.L. Pedano, M.D. Rubianes, M.T. Martínez, G. Rivas, Electroanalysis 26 (2014) 1676–1683.
[18] C.G. Salzmann, M.A.H. Ward, R.M.J. Jacobs, G. Tobias, M.L.H. Green, J. Phys. Chem. C 111 (2007) 18520.
[19] T. Higashi, Y. Nakajima, M. Kojima, K. Ishii, A. Inoue, T. Maekawa, T. Hanajiri, Chem. Phys. Lett. 501 (2011) 451–454.
[20] T. Tsoufis, A. Ampoumogli, D. Gournis, V. Georgarilas, L. Jankovic, K.C. Christoforidis, Y. Deligiannakis, A. Rudolf, A. Mateo-Alonso, M. Prato, Carbon 67 (2014) 433.
[21] M. Kojima, T. Chiba, J. Niishima, T. Higashi, T. Fukuda, Y. Nakajima, S. Kurosv, T. Hanajiri, K. Ishii, T. Haekawa, A. Inoue, Nanoscale Res. Lett. 6 (2011) 1–6.
[22] J.M. González-Domínguez, F.A. Gutierrez, J. Hernández-Ferrer, A. Ansón-Casaos, M.D. Rubianes, G. Rivas, M.T. Martínez, J. Mater. Chem. B 3 (2015) 3870–3884.
[23] M. Naczk, F. Sahidi, J. Pharm. Biomed. Anal. 41 (2006) 1523.
[24] R.M. Muir, A.M. Ibáñez, S.L. Uratsu, E.S. Ingham, C.A. Leslie, G.H. McGranaham, N. Batra, S. Goyal, J. Joseph, E.D. Jernnis, A.M. Dandekar, Plant. Mol. Biol. 75 (2011) 535–565.
[25] B. Boye, E. Brillas, A. Buso, G. Farnia, M. Giomo, G. Sandon, Elect. Acta 52 (2006) 256–262.
[26] I. Madnic, D. Modun, V. Rastija, J.W. Kovic, I. Brizic, V. Katalinic, B. Kozina, M. MedicSaric, M. Boban, Food Chem. 119 (2010) 1205–1210.
[27] S.M. Ghoreishi, M. Behpoor, M. Khayatkashani, M.H. Motaghedifard, Anal. Methods 3 (2011) 636–645.
[28] J. Tashkhourian, S.F. Nami-Ana, Mater. Sci. Eng. C 52 (2015) 103.
[29] J. Tashkhourian, S.F. Nami Ana, S. Hashemnia, M.R. Hormozi-Nezhad, J. Solid State Electrochem. 17 (2013) 157.
[30] M. Kahl, T.D. Golden, Electroanalysis 26 (2014) 1664.
[31] P. Jara-Ulloa, P. Salgado-Figueroa, R. Moscoso, J.A. Squella, J. Electrochem. Soc. 160 (2013) H243.
[32] R. Abdel-Hamid, E.F. Newair, J. Electroanal. Chem. 704 (2013) 32.
[33] N.S. Sangeetha, S.S. Narayanan, Anal. Chim. Acta 828 (2014) 34.
[34] L.P. Souza, F. Calegari, A.J.G. Zarbin, L.H. Marcolino-Junior, M.F. Bergamini, J. Agric. Food Chem. 59 (2011) 7620.
[35] S.M. Ghoreishi, M. Behpour, M. Khayatkashani, M.H. Motaghedifard, Anal. Meth. 3 (2011) 636.
[36] M. Di Fusco, C. Tortolini, D. Deriua, F. Mazzeia, Talanta 81 (2010) 235.
[37] M. Amatatongchai, W. Sroysee, S. Laosing, S. Chairam, Int. J. Electrochem. Sci. 8 (2013) 10526.
[38] M. Gamella, S. Campuzano, A.J. Reviejo, J.M. Pingarrón, J. Agric. Food. Chem. 54 (2006) 7960–7967.
[39] J. Coates, in: R.A. Meyers (Ed.), Encyclopedia of Analytical Chemistry, John Wiley & sons Ltd., Chichester, 2000, p. 10815.
[40] C.N.R. Rao, Chemical Applications of Infrared Spectroscopy, 1963 (New York and London).
[41] Y. Wang, C. Bi, J. Mol. Liq. 177 (2013) 26.
[42] Y. Liu, L. Yu, S. Zhang, J. Yuan, L. Shi, L. Zheng, Colloid. Surf. A 359 (2010) 66.
[43] Z. Wu, W. Feng, Y. Feng, Q. Liu, X. Xu, T. Sekimo, A. Fujii, M. Ozaki, Carbon 45 (2007) 1212.
[44] J. Yu, N. Grossiord, C.E. Koning, J. Loos, Carbon 45 (2007) 618.
[45] F. Lu, S. Zhang, L. Zheng, J. Mol. Liq. 173 (2012) 42.
[46] A. Escarpa, M.C. González, Anal. Chim. Acta 427 (2001) 119.
[47] B.B. Petković, S. Stanković, M. Milčić, S.P. Sovilj, D. Manojlović, Talanta 132 (2015) 513.
[48] J. Tashkhourian, S.F. Nami-Ana, Mater. Sci. Eng. C 52 (2015) 103.
[49] J. Tashkhourian, S.F. Nami Ana, S. Hashemnia, M.R. Hormozi-Nezhad, J. Solid State Electrochem. 17 (2013) 157.
[50] M. Kahl, T.D. Golden, Electroanalysis 26 (2014) 1664.
[51] P. Jara-Ulloa, P. Salgado-Figueroa, R. Moscoso, J.A. Squella, J. Electrochem. Soc. 160 (2013) H243.
[52] R. Abdel-Hamid, E.F. Newair, J. Electroanal. Chem. 704 (2013) 32.
[53] N.S. Sangeetha, S.S. Narayanan, Anal. Chim. Acta 828 (2014) 34.
[54] L.P. Souza, F. Calegari, A.J.G. Zarbin, L.H. Marcolino-Junior, M.F. Bergamini, J. Agric. Food Chem. 59 (2011) 7620.
[55] S.M. Ghoreishi, M. Behpour, M. Khayatkashani, M.H. Motaghedifard, Anal. Meth. 3 (2011) 636.
[56] J.H. Luo, B.L. Li, N.B. Li, H.Q. Luo, Sensors Actuat. B 186 (2013) 84.
[57] M. Di Fusco, C. Tortolini, D. Deriua, F. Mazzeia, Talanta 81 (2010) 235.
[58] M. Amatatongchai, W. Sroysee, S. Laosing, S. Chairam, Int. J. Electrochem. Sci. 8 (2013) 10526.
[59] W. Ma, D. Han, S. Gan, N. Zhang, S. Liu, T. Wu, Q. Zhang, X. Donga, L. Niua, Chem. Commun. 49 (2013) 7842.
[60] I.L. de Mattos, J.H. Zagal, Int. J. Anal. Chem. (2010) 143714, 1.
[61] S.G. Dmitrienko, O.M. Medvedeva, A.A. Ivanov, O.A. Shpigun, Y.A. Zolotov, Anal. Chim. Acta 469 (2002) 295.
[62] M.E. Yue, T.F. Jiang, Y.P. Shi, J. Anal. Chem. 61 (2006) 365.
[63] W. Samee, S. Vorarat, Thai. Pharm. Health Sci. J. 2 (2007) 131.